Title
Effects of myelin or cell body brainstem lesions on 3-channel Lissajous' trajectories of feline auditory brainstem evoked potentials.

Journal
Hearing research, 53(2)

ISSN
0378-5955

Authors
Pratt, H
Zaaroor, M
Bleich, N
et al.

Publication Date
1991-06-01

DOI
10.1016/0378-5955(91)90058-h

Hearing Research, 53 (1991) 237–252

HEARES 01566

Effects of myelin or cell body brainstem lesions on 3-channel Lissajous' trajectories of feline auditory brainstem evoked potentials

H. Pratt, M. Zaaroor, N. Bleich and A. Starr [1]

Evoked Potentials Laboratory Technion – Israel Institute of Technology, Haifa, Israel and [1] Department of Neurology, University of California, Irvine, California, U.S.A.

(Received 6 August 1990; accepted 12 December 1990)

Auditory brainstem evoked potentials (ABEP) were recorded from 16 awake cats to obtain 3-Channel Lissajous' Trajectories (3CLTs) using three orthogonal differential electrode configurations (nasion – midline nuchal ridge, left – right mastoids, vertex – midline under the mandible). Potentials, evoked by monaural 80 dBnHL (re. human threshold) clicks, were studied before, and up to 7 weeks after inducing neuronal lesions localized to the cochlear nucleus (CN) or the superior olivary complex (SOC), or myelin lesions localized to the fibers of the trapezoid body connecting these two structures. Neuronal lesions were induced by injection of kainic acid (KA), while myelin lesions were induced by injection of L-alpha-lysophosphatidylcholine (LPC).

With CN neuronal lesions the major changes in 3CLT were in the time domain of 'b', 'c' and 'd' (components P2, P3 and P4 of single-channel ABEP). With SOC neuronal lesions the major changes were in 'c' and 'd' of 3CLT (P3 and P4 of ABEP). With trapezoid body lesions the major change was in 'c' (P3 of ABEP).

The results are compatible with the peripheral generation of the first ABEP components (P1a and P1b). The second component (P2) is generated by ipsilateral CN neurones and their outputs. The third component (P3) is generated primarily by ipsilateral SOC neurones and their outputs, with the ipsilateral CN providing input. The fourth component (P4) is generated bilaterally by the SOC neurones and their outputs, receiving their inputs from ipsilateral CN. The fifth ABEP component (P5) is generated by structures central to the SOCs and their immediate outputs.

Neither focal neuronal nor myelin lesions were sufficient to produce obliteration of any component, consistent with a set of generators for each of the ABEP components, consisting of both cell bodies and their output fibers, that is distributed spatially in the brainstem.

Auditory brainstem evoked potentials; 3CLT; Myelin lesions; Neuronal lesions; Cochlear nucleus; Superior olivary complex; Trapezoid body

Introduction

The generators of surface recorded auditory brainstem evoked potentials (ABEP) have been the subject of numerous studies (in humans: Møller et al., 1981, 1988; Hashimoto et al., 1981; Møller and Jannetta, 1982, 1985; Curio et al., 1987; and in animals: Lev and Sohmer, 1972; Achor and Starr, 1980a; Caird et al., 1985; Legatt et al., 1986a,b; Kano and Starr, 1987; Møller and Burgess, 1986; Starr and Zaaroor, 1990; Buchwald and Huang, 1975; Achor and Starr, 1980b; Wada and Starr, 1983a,b,c; Gardi et al., 1987; Zaaroor and Starr, in press a,b). All of the studies have correlated intracranial activity or the effects of brainstem lesions with the surface recorded ABEP, usually derived from a single pair of electrodes. Such correlations are complicated by the effects of surface electrode position on the latency and amplitude of the components (Picton et al., 1974; Plantz et al., 1974; Allen and Starr, 1978; Prasher and Gibson, 1980; Starr and Squires, 1982; Wada

Correspondence to: H. Pratt, Evoked Potentials Laboratory, Technion – Israel Institute of Technology, Haifa 32000, Israel.

and Starr, 1983a,b). The three-channel Lissajous' trajectory (3CLT) of evoked potentials (Williston et al., 1981; Pratt et al., 1983), affords a concise representation of the surface reflection of auditory brainstem activity, independent of electrode position relative to generators (Martin et al., 1987b). In 3CLT each data point represents the simultaneous voltage values from three orthogonal electrode pairs, which can be considered isomorphic with the tip of a centrally located equivalent dipole moment, that changes magnitude and orientation over time (Pratt et al., 1983; Scherg, 1984). 3CLT may provide insights for understanding the generation of auditory brainstem evoked potentials (Pratt et al., 1987; Gardi et al., 1987).

Two types of neural processes have been proposed as generating ABEP: 1) Fiber tract discharges (Jewett and Williston, 1971; Nunez, 1981; Starr and Squires, 1982; Wada and Starr, 1983c; Legatt et al., 1986b; Rudell, 1987; Ozdamar and Delgado, 1990) at changing impedance boundaries (Nakanishi, 1982; Kimura et al., 1984) or at points of curvature (Deupree and Jewett, 1988); 2) neural synaptic events (Buchwald, 1983). These suggestions have been based on indirect experimental evidence, or lesions which affect both fibers of passage and neurons (e.g., aspiration of brain structures, electrolytic lesions).

In this study we examined the effects of specific lesions to myelin (Hall and Gregson, 1971; Gregson and Hall, 1973; Hall, 1983) or cell bodies (Coyle et al., 1978) induced by injection of L-alpha-lysophosphatidyl-choline (LPC) or kainic acid (KA), respectively, to the cochlear nucleus (CN) or superior olivary complex (SOC) of cats. In order to avoid the complications introduced by position of the recording electrodes, the effects of these lesions on 3CLTs, rather than single-channel records, of ABEP were analyzed.

Methods

Normative data were obtained from 16 adult cats (2500–3400 g); five of which were subsequently injected with LPC to the left trapezoid body in the vicinity of SOC, five were injected with KA into the left CN, and five with KA into the left SOC. In addition to these unilateral lesions, one cat was injected with KA to the SOC,

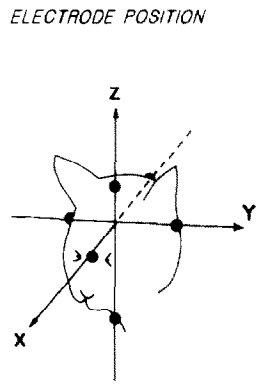

Fig. 1. Electrode positions and recording configurations for feline 3CLT analysis. The arrows point toward positive values in each axis.

bilaterally. Prior to each recording session, cats were otoscopically examined to rule out conductive hearing loss due to mites or ear infections.

In order to avoid possible effects of anaesthesia and body temperature changes, potentials were recorded with the cat awake in a restraining bag. Subdermal needle electrodes were arranged in 3 differential derivations (Fig. 1): over frontal sinus - back of the neck (labeled 'X'), left-right mastoids (labeled 'Y') and vertex - mid-line under the mandible (labeled 'Z'). The 'X' derivation was not precisely at right angles to the 'Y' and 'Z' channels and the data were subsequently adjusted mathematically to correct for this discrepancy. A grounding screw was placed in the left frontal sinus with its head inverted through a small key hole. The interelectrode impedance was measured with a sine-wave impedance meter and verified to be 5 kΩ or less. Potentials from each of the 3 channels were differentially amplified (×100 000) at a band pass of 30–3000Hz (−3 dB points, 6 dB/octave slopes). The amplified potentials were averaged (12 bit analog-to-digital converter) using 512 addresses and a dwell time of 20 μs per point per channel. When cats were relaxed the amplified potentials spanned 50% of the analog-to-digital converter's range. Sweeps that included potentials that approached the full range were not included in the average.

Stimuli were clicks generated by transducing 100 μs square electric pulses in Sony MDR-E225 dynamic earphones positioned to be just outside the external auditory meatus. Clicks were pre-

sented to each ear in turn. Potentials following 4000, 80 dB nHL (re. normal human threshold, 115 dB impulse SPL), condensation clicks presented at a rate of 10.6/s were averaged to produce each trace. The averaged 3-channel data were magnetically stored for further analysis.

Details of the surgical and lesion induction procedures were provided elsewhere (Zaaroor and Starr, 1991a,b). In brief, a microelectrode, both for recording potentials at its tip and for transmitting KA or LPC into the brainstem, was filled with a 1% solution of the appropriate substance (KA or LPC), and lowered into the structure to be lesioned. Position of the electrode tip, during surgery, was determined visually through the operating microscope, as well as electrophysiologically. KA, or LPC, was injected over 30 min to attain a total volume of 0.5 μl for KA and up to 14 μl for LPC. Both acute and chronic effects of the lesions were studied by repeat ABEP recordings up to 45 days after lesion induction.

At the end of the experimental sessions the animal was deeply anesthetized with sodium pentobarbital (100 mg/kg) and perfused with normal saline followed by 10% buffered formalin. Frozen sections of the brainstem, were cut and stained with crystal violet for cell bodies and with Kluver Barrera stain or Chromoxane Cyanine R with crystal violet for myelin. The extent of neuronal loss (in KA lesions), or myelin loss (with LPC lesions), was defined, with the aid of a camera lucida, by calculating the area of the lesion on both the injected and intact side of the brainstem. Up to three fields in each subdivision of the SOC or CN were examined, and these numbers were averaged across sections. The identity of the cat was known to the person performing the histology (M.Z.). However, 3CLT analysis was performed by another person (N.B.) without knowledge of the extent of lesion, using a machine-scoring algorithm which is free of experimenter's bias.

Details of the 3CLT analysis are provided in Appendix 1. In brief, following digital filtering (Finite Impulse Response filter, Urbach and Pratt, 1986) to a bandpass of 100–3000 Hz and mathematical adjustment of the 'X' channel data to orthogonality with the 'Y' and 'Z' channels' data, 3CLTs were obtained and analyzed. Analysis related to point-by-point (local) attributes of the trajectory, as well as segmental (global) attributes. Points where both the local rate of bending of the trajectory in voltage space and the distance from the origin (trajectory amplitude) were locally maximal were defined as apices. Sequences of points along the trajectory whose root-mean-square distance from a best-fitting plane was under 0.1 μV were defined as planar segments. Intersubject variability of planar segment (or apex) orientation was calculated in terms of the average angles ('included angles') by which individual planar segment (or apex) orientations deviated from the average orientation.

Data analysis

The 3CLT measures used in this study were apex latency, amplitude and orientation, as well as planar segment onset latency, duration and orientation. Amplitude of a component is proportional to the number of synchronously firing neural elements in its generator. It is therefore reasonable to assume that decreasing the number of neural elements (neurones or fibers) in a generator, by a lesion, would result in a proportional decrease in amplitude. Similarly, latency is expected to be prolonged by lesions as a result of either longer rise times in synaptic potentials resulting from decreasing number of presynaptic neurones or delayed conduction along demyelinated fibers. This rationale is basic to the wide spread clinical utility of evoked potentials amplitudes and latencies. In this study, statistical evaluation included multiple regression analyses, where the dependent variable was the 3CLT descriptor studied (apex latency or amplitude, planar segment onset latency or duration) and the independent variables – time since lesion induction and the extent of lesion in the right and left anterior ventral cochlear nucleus (AVCN), posterior ventral cochlear nucleus (PVCN), dorsal cochlear nucleus (DCN), medial nucleus of the trapezoid body (MNTB), lateral superior olivary nucleus (LSO) and medial superior olivary nucleus (MSO).

Regressions that proved significant by ANOVA ($P < 0.05$ for slopes of 0), and which also included a significant time-since-lesion coefficient were considered indicative of effects of the lesioned structure (as opposed to acute, non-specific effects of surgery such as edema). Because time-since-le-

sion and the extents of lesions were independent variables, the combined significance level achieved with this criterion was 0.0025, compensating for the multiple regression analyses performed (9 components × 4 3CLT measures). In another analysis, a paired *t*-test procedure was used to compare 3CLT measures (apex latency or amplitude, planar segment onset latency or duration) before and 7 days after lesion induction. Because multiple *t*-tests were performed (9 components × 4 3CLT measures), with the Bonferroni correction, only probabilities that were lower than 0.001 were considered significant, and lower than 0.009, marginally significant. Pre- vs. post-lesion changes in apex or planar segment orientations were considered significant if larger than the 90% limits of

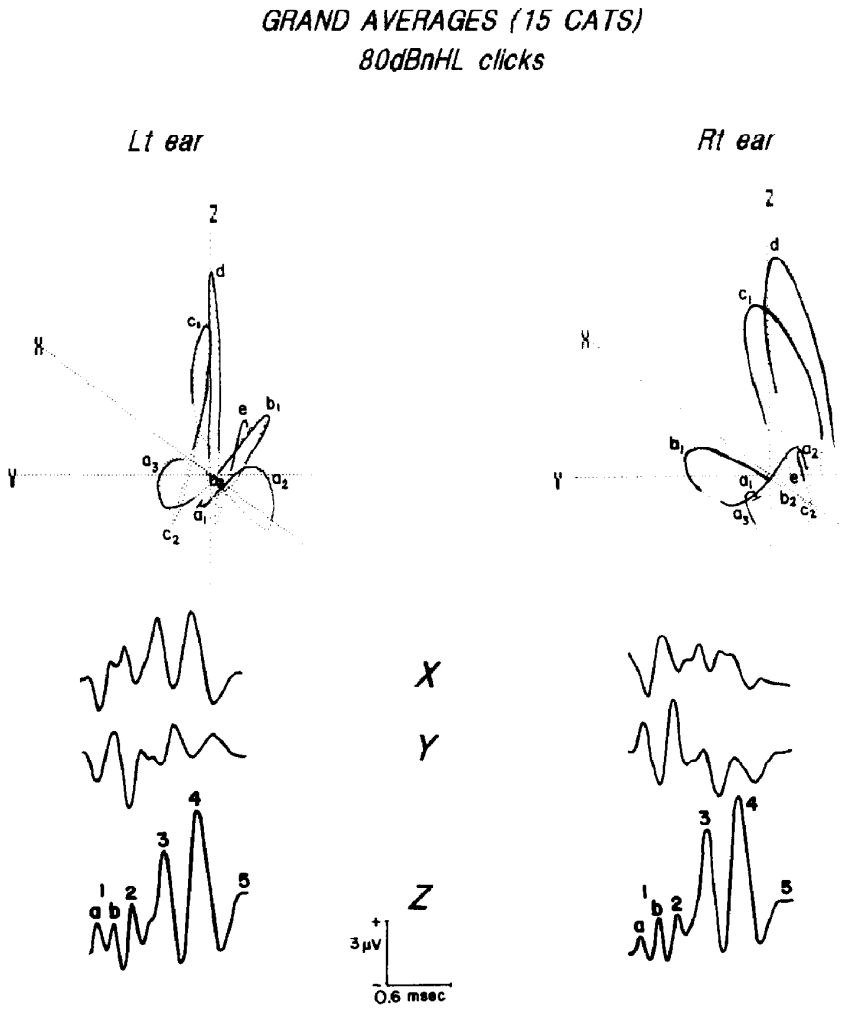

Fig. 2. 3CLTs of ABEP, to left and to right ear stimulation, before lesion induction, averaged across 15 cats, with the 'X', 'Y' and 'Z' records from which they were derived. The 3CLT included 5 loops, which roughly corresponded in their latency to the 'Z' channel components 1 through 5. These loops were labeled 'a' through 'e', respectively. When more than one plane was identified in a loop, the planes were given numerical descriptors, in the order of their appearance (e.g. 'c1', 'c2' etc.). In order to enhance differentiation between successive planar segments, they are plotted in solid or dotted lines, alternatingly.

the pre-lesion orientation variability, which being two tailed, corresponds to beyond the mean ±2 SD limits in normally distributed variables.

Results

The variability of single-channel records, as well as 3CLTs, across cats was remarkably small. Comparing waveforms or 3CLTs averaged across all cats, with those averaged across subsets of the cat population, or with data from individual cats showed very little differences (e.g., compare Fig. 2 'Rt ear' with Figs. 3, 5 and 7 'contralateral' or with Fig. 6 'pre-lesion'). We have therefore chosen to demonstrate waveforms and 3CLTs as averages across animals, and to provide the variability of measures in the Tables. Two instances of individual cat data are included to demonstrate the effects of the largest lesions.

Pre-lesion

The ABEP of the cat consists of 5 major peaks – labelled '1' to '5', best seen in the 'Z' channel records. Peak '1' can be subdivided into two subpeaks '1a' and '1b'. The 3CLT of ABEP averaged across all cats ($N = 15$) is presented in Fig. 2, with the 'X', 'Y' and 'Z' records. The 3CLT included 5 loops ('a' to 'e'), which corresponded in their time domains to the 5 peaks in the 'Z' channel. When more than one plane was identified in a loop, the planes were given numerical descriptors, in the order of their appearance (e.g. 'c1', 'c2' etc.). The normative, pre-lesion, 3CLT measures analyzed in this study are listed in Table I for apex attributes and in Table II for planar segment attributes. The peaks, as defined in the 'Z' channel, are placed below the respective 3CLT components. Average orientation variabilities (AOVa or AOVp) are provided to complement limits of orientation variability (LOVa and AOVp) as indicators of orientation variabilities, but were not used in the statistical evaluation. Note that the normal orientation variability (LOVa in Table I) changes between apices from 18° (average 15°) for 'c1' to 91° (average 52°) for the 'a3' apex. The planes (LOVp in Table II) consistently display larger variabilities ranging

TABLE I

NORMATIVE APEX MEASURES OF FELINE 3CLT COMPONENTS

3CLT	a1	a2	a3	b1	b2	c1	c2	d	e
Z Correlates		1a	1b	2		3		4	5
both ears									
LATa	0.7±0.1	1.1±0.1	1.4±0.1	1.7±0.1	2.0±0.1	2.4 ±0.1	2.7±0.1	3.2 ±0.2	4.0±0.3
AMPa	4.2±2.3	8.2±3.2	7.7±3.5	9.4±2.4	3.9±2.2	16.0±7.6	8.7±3.7	19.0±5.7	7.7±2.3
AOVa	30	35	52	31	73	15	58	12	50
LOVa	47	51	91	61	77	18	47	21	81
right ear									
Aa	0.31	−0.67	0.71	0.48	−0.44	−0.07	0.24	−0.14	−0.70
Ba	0.39	0.26	−0.50	0.73	−0.87	−0.03	−0.39	−0.02	0.05
Ca	−0.87	−0.69	−0.51	0.49	−0.22	1.00	−0.89	0.99	0.71
left ear									
Aa	0.15	−0.85	0.68	0.15	−0.16	0.08	0.14	−0.08	−0.69
Ba	0.00	−0.52	0.40	−0.61	0.50	−0.07	0.40	0.01	0.09
Ca	−0.99	−0.03	−0.62	0.77	0.85	0.99	−0.91	1.00	0.72

Orientation coefficients are listed separately for responses to left and right ear stimulation. Standard deviations are preceded by ±. Peaks in the 'Z' channel are placed under the 3CLT components corresponding in latency. The method of obtaining these measures is outlined in the Appendix.

LATa – apex onset latency (in ms); AMPa – apex amplitude (in μV); AOVa – average intersubject orientation variability (degrees of included angle); LOVa – 90% limit of apex orientation variability (degrees of included angle); Aa, Ba and Ca – cosines with analysis axes 'X', 'Y' and 'Z', respectively.

TABLE II

NORMATIVE PLANAR MEASURES OF FELINE 3CLT COMPONENTS

3CLT	a1	a2	a3	b1	b2	c1	c2	d	e
Z Correlates		1a	1b	2		3		4	5
both ears									
LATp	0.4±0.3	0.9±0.1	1.3±0.1	1.5±0.1	1.8±0.1	2.2±0.1	2.5±0.2	2.9±0.2	3.6±0.3
DURp	0.4±0.2	0.3±0.1	0.3±0.1	0.3±0.1	0.3±0.1	0.5±0.1	0.4±0.2	0.6±0.3	0.8±0.3
AOVp	77	42	44	73	76	38	54	60	57
LOVp	79	80	82	80	78	50	74	73	79
right ear									
Ap	0.23	−0.86	0.75	−0.16	−0.81	0.61	0.66	0.14	−0.99
Bp	0.37	−0.05	−0.57	0.33	−0.54	−0.69	−0.64	−0.96	−0.01
Cp	−0.74	0.51	0.34	−0.93	0.23	0.40	0.39	0.26	0.14
Dp	0.82	1.00	0.80	0.86	0.28	2.60	1.11	0.78	1.37
left ear									
Ap	0.27	−0.82	0.96	−0.35	−0.87	0.56	0.10	−0.38	−1.00
Bp	0.54	−0.10	0.15	−0.57	0.28	0.68	0.92	−0.09	0.04
Cp	−0.80	0.56	0.24	−0.75	0.40	0.47	0.38	0.39	0.06
Dp	0.17	1.20	1.57	1.51	0.48	1.58	0.57	0.55	1.29

Orientation coefficients are listed separately for responses to left and right ear stimulation. Standard deviations are preceded by ±. Peaks in the 'Z' channel are placed under the 3CLT components corresponding in latency. The method of obtaining these measures is outlined in the Appendix.

LATp – planar onset latency (in ms); DURp – planar duration (in ms); AOVp – average intersubject orientation variability (degrees of included angle); LOVp – 90% limit of planar orientation variability (degrees of included angle); Ap, Bp and Cp – cosines with analysis axes 'X', 'Y' and 'Z', respectively; Dp – plane position (length of sight-vector, in μV).

from 50° (average 38°) for 'c1' to 82° (average 44°) for 'a3'. Deviations beyond these (LOV) values will be considered significant.

Neuronal lesions

The effects of neuronal destruction of the left CN on 3CLTs averaged across cats are shown in Fig. 3. There were marked changes when stimulation was ipsilateral to the lesioned side consisting of the absence of loop 'b', a change in shape of 'c', while the other components, 'd' and 'e', were preserved. Apex latencies were practically identical bilaterally. In the 'Z' record to ipsilateral stimulation, peaks 1a, 1b, 4 and 5 are essentially unaffected while the interposed peaks 2 and 3 are markedly attenuated. The data from the cat with a near total destruction of the left CN (cat 21) is presented in Fig. 4. 3CLT following the lesion showed substantial prolongation of apex latencies beginning with 'b', marked attenuation and orientation changes of 'b' and 'c', and relative preservation of 'a' and 'd'.

The effect of neuronal lesions to the left superior olive on 3CLT to contralateral and ipsilateral stimulation, averaged across cats, is shown in Fig. 5. There is a decrease in apex amplitudes of 'd' relative to 'c', with ipsilateral stimulation compared to contralateral stimulation. This effect is parallelled by the relative amplitude changes in peaks 3 and 4 of the respective 'Z' channel records. Apex latencies were not affected by these lesions.

In one cat (cat 20), the neurones of the superior olivary complex were bilaterally destroyed. This lesion resulted in changes (Fig. 6) in apex orientation of 'a' and 'b', and apex amplitude reductions of 'c' and 'd', corresponding to the attenuation of peaks 3 and 4 in the 'Z' channel record.

Myelin lesions

3CLTs to stimulation of the ear ipsi- and contralateral to myelin lesion of the trapezoid body in the vicinity of the left superior olive revealed only a minor orientational change of 'c' to ipsilateral stimulation without a corresponding change in the 'Z' channel record (Fig. 7). Apex latencies were not affected.

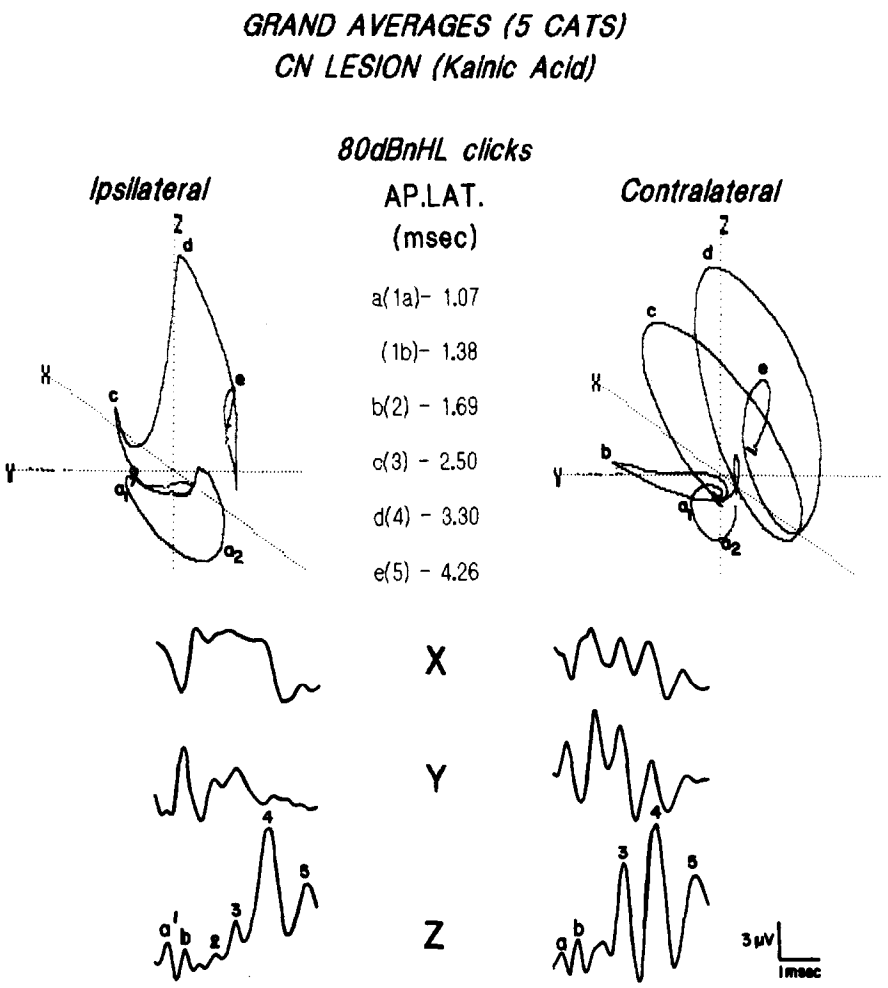

Fig. 3. 3CLTs of ABEP to stimulation of ipsi- and contralateral ear following neuronal destruction in the CN, averaged across 5 cats. Note the marked changes when stimulation was ipsilateral to the lesioned side. In the 3CLT to ipsilateral stimulation, note the disappearance of 'b', the shape change in 'c' and the relative preservation of the other components. Apex latencies (AP.LAT) were the same for both records.

Data from all three types of lesions were analyzed for significant apex orientation changes, expressed as the ratio between cats with a significant (beyond the 90% pre-lesion variability) change and the total number of cats with that type of lesion (Table III). The apex orientations of 'a2', 'b1' and 'c1' were affected by the lesions in the majority of the cats. No correlation between extent of lesion at the various subdivisions of each structure (Table IV) and the amount of orientational changes could be established. No significant changes in planar segment orientations were observed following lesions.

The effects of the extent of lesions on the apices and planes were evaluated by multiple regression analysis. Table V summarizes the significant effects and their directions (increase or decrease). In general, with the exception of one planar measure (LATp), only apical measures (noted by 'a') were sensitive to lesions. Significant effects of lesions resulted in latency increases (with only one exception), while effects on amplitudes varied, depending on the lesioned structure: MNTB lesions resulted in apex amplitude decrease, while MSO and LSO lesions resulted in apex amplitude increases.

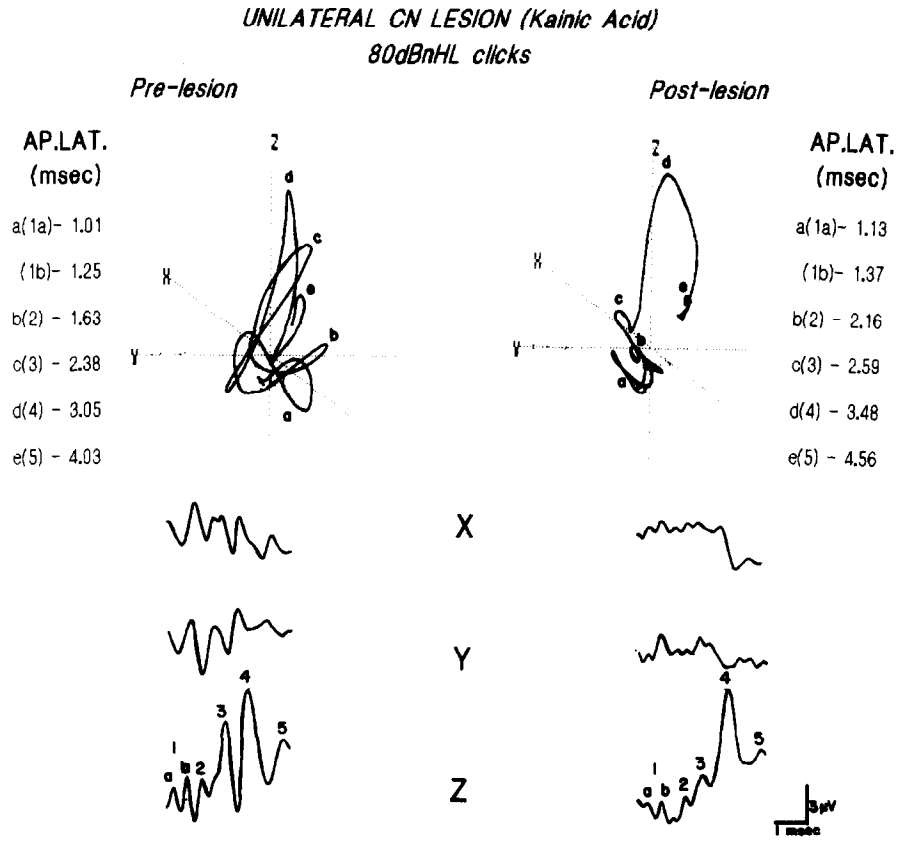

Fig. 4. 3CLTs in response to left ear stimulation from a cat with a near total neuronal destruction in the left CN, before and after lesion induction. There are changes in apex latencies (AP.LAT.) and the components following 'a'.

There were significant post- vs. pre-lesion differences in 3CLT apex measures (Table VI). Ipsilateral lesions were more effective than contralateral lesions in producing changes. In contrast to the numerous effects on apical measures listed in Table VI, only the onset latency of planar

TABLE III

INCIDENCE OF SIGNIFICANT APEX ORIENTATION CHANGES FOLLOWING BRAINSTEM LESIONS

3CLT	a1	a2	a3	b1	b2	c1	c2	d	e
Z Correlates		1a	1b	2		3		4	5
Kainic Acid									
CN	1/5	3/5	0/5	3/5	1/5	4/5	2/5	0/5	0/5
SOC	1/5	0/5	0/5	3/5	1/5	3/5	2/5	1/5	1/5
Lyso. Phosph. Chol.									
SOC	0/5	3/5	1/5	2/5	2/5	2/5	1/5	0/5	1/5

Incidence is given as the number of cats with significant orientational change out of the total number of cats with this type of lesion. Peaks in the 'Z' channel are placed under the 3CLT components corresponding in latency.

CN – lesion to cochlear nucleus; SOC – lesion to superior olivary complex.

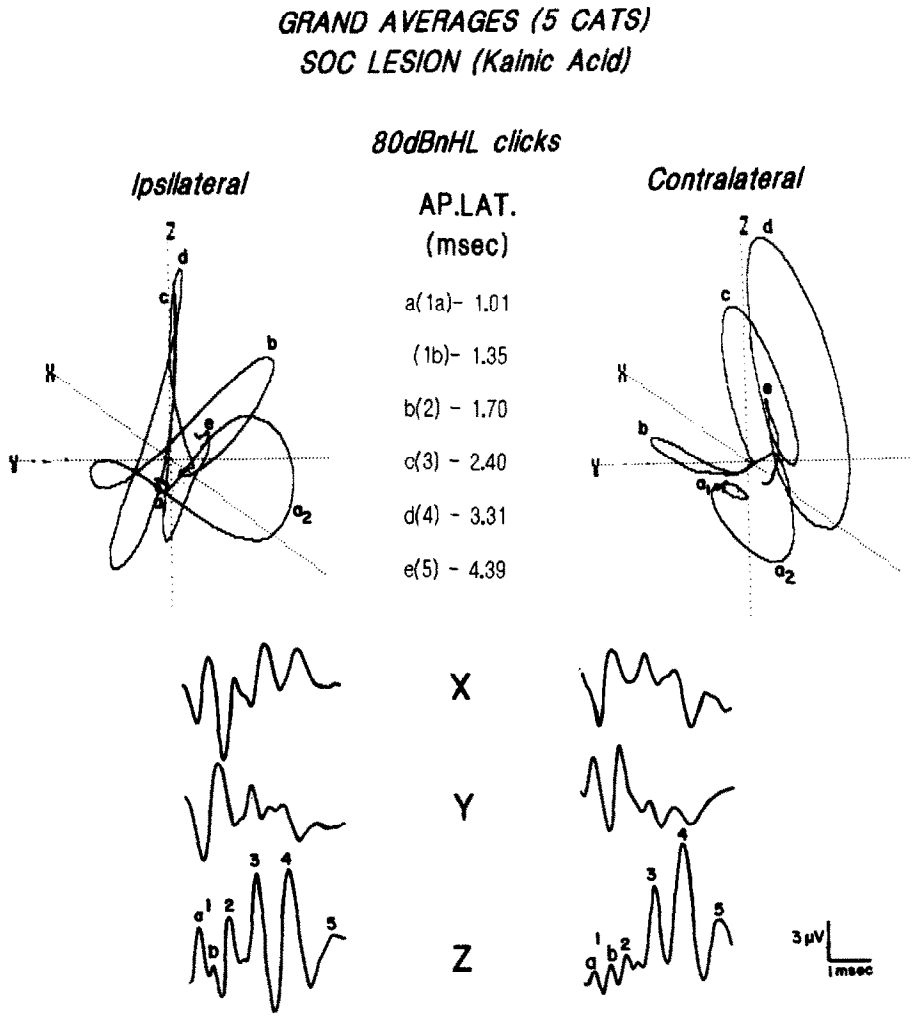

Fig. 5. 3CLTs of ABEP to stimulation of ipsi- and contralateral ear following neuronal destruction in the SOC, averaged across 5 cats. There is some decrease in the relative amplitude of 'd' relative to 'c' in response to ipsilateral stimulation, also evident in the 'Z' channel record. Apex latencies (AP.LAT.) were the same for both records.

segment 'd' was significantly delayed following neuronal lesions to CN or SOC, and onset latency and duration of planar segment 'e' increased as a result of myelin lesions to SOC.

Discussion

The results of this study of 3CLT of the cat auditory brainstem evoked potentials showed that all apex measures of many components were sensitive to both neuronal and myelin lesions. There were orientational changes, latency increases, and amplitude changes which varied, depending on the lesioned structure. In contrast, only the onset latency of planar segment 'd' and the onset latency and duration of planar segment 'e' changed significantly following lesions. The difference in sensitivity to brainstem lesions between apical and planar measures suggests that apex measures are more directly related to the functional integrity of ABEP generators. The finding that myelin lesions of trapezoid body affected only planar attributes

may be related to the suggestion that planar segments are generated by curving fiber tracts (Pratt et al., 1987; Chimento et al., 1987). *

We suggest that lesions of the auditory brainstem pathway affect 3CLT measures in the following manner: Amplitude changes (increase or decrease) reflect a change (i.e. increase or decrease) in synchronized activity of the neural elements responsible for the affected component. Changes in orientation, without amplitude effects, reflect alterations in a subset of the neural elements responsible for the affected component. Latency prolongation reflects alterations peripheral to the generator of the affected component.

With CN lesions, the earliest changes in 3CLT included orientation change of 'a2' (3 out of 5 animals) and latency increase of 'a3' that correlated with the extent of lesions of both the PVCN and the LSO. Components 'a2' and 'a3' are equivalent to peaks 1a and 1b in the 'Z' channel and reflect activity of the VIII nerve (Starr and Zaaroor, 1990). Changes in their 3CLT measures may result from chronic central auditory pathway lesions affecting the excitability of the VIII nerve. Such an effect could result from changes either in efferent activity to the cochlea that originates in the SOC, or changes in the excitability of VIII nerve fibers due to a loss of their terminal sites in CN (Von Monakow, 1914).

Component 'b1', corresponding to P2 in the 'Z' channel ABEP, to ipsilateral stimulation had a change in apical orientation (3 of 5 cats with both CN and SOC neuronal lesions) and an amplitude reduction and latency increase with CN neuronal lesions. These results are compatible with CN neurones and their outputs as the major contributors to 'b'. The orientation changes of b1 with SOC neuronal lesions indicate that this structure also participates to a minor degree in the generation of this component.

Component 'c1', corresponding to P3 of the 'Z' channel ABEP, to stimulation of the ipsilateral ear, had changes in orientation with CN (4 of 5 cats) and SOC (3 of 5 cats) neuronal lesions. Compared to pre-lesion records, its amplitude decreased and latency increased with CN lesions whereas with SOC lesions these measures were not affected (Table VI). The lack of change of amplitude with SOC lesions can probably be attributed to the finding that the amplitude of 'c1' changed in opposite directions depending on the specific subnucleus of the SOC affected. Thus, 'c1' amplitude increased with the extent of the lesion of LSO and decreased with the extent of the lesion of MNTB (Table V). These results indicate that the ipsilateral MNTB and the LSO interact as the major contributors to this component and that ipsilateral CN provides their input.

Component 'd', corresponding to P4 of the 'Z' channel ABEP, showed an amplitude decrease with ipsilateral SOC neuronal lesions and both an amplitude decrease and a latency increase to ipsilateral CN neuronal lesions (Table VI). 'd' amplitude increased with the extent of lesion of both ipsilateral and contralateral MSO, of ipsilateral LSO, and decreased with the extent of lesion of the ipsi- and contralateral MNTB (Table V). The effects of CN lesions on 'd' were the same as on

* There are several methodological differences between the present study and that of Martin et al. (1987a) which could account for minor differences in normative results. The present machine-scoring procedure, using strict rules for apex and plane definition, defined 9 apices and associated planes, as compared to 12 in the manually defined components of Martin et al. (1987a). In order to compare homologous components between the two studies, differences in methodology need to be outlined. In the present study condensation clicks presented directly to the ear canal at 115 dB impulse SPL were used, compared to rarefaction clicks, presented through an earbar at 70 dB impulse SPL. Another source of difference between studies may be the recording highpass. Martin et al. used analog filters with a high-pass of 10 Hz whereas in our study the waveforms were digitally filtered with a high-pass of 100 Hz. This difference would particularly affect the later components, which temporally overlap the slow 'pedestal'. Comparing stimulus waveforms and timing, taking the intensity differences into account and accounting for possible effects of recording passbands on the later components, the latencies in the present study can be expected to be shorter by 0.2–0.5 ms compared to Martin et al.'s results. Thus, the present 'a1' component has no corresponding component in Martin et al.'s report, while their components 'c1', 'c2', 'd1' and 'd4' have no corresponding components in the present study. Otherwise, this study's components 'a2', 'a3', 'b1', 'b2', 'c1', 'c2', 'd' and 'e' correspond to Martin et al.'s components 'a1', 'a2', 'b1', 'b2', 'c3', 'c4', 'd2' and 'd3'. This interpretation is supported by the larger orientation variabilities of segments 'c1', 'c2', 'd1' and 'd4' (which have no counterparts in our study), relative to the other segments of that study (which did correspond to our segments).

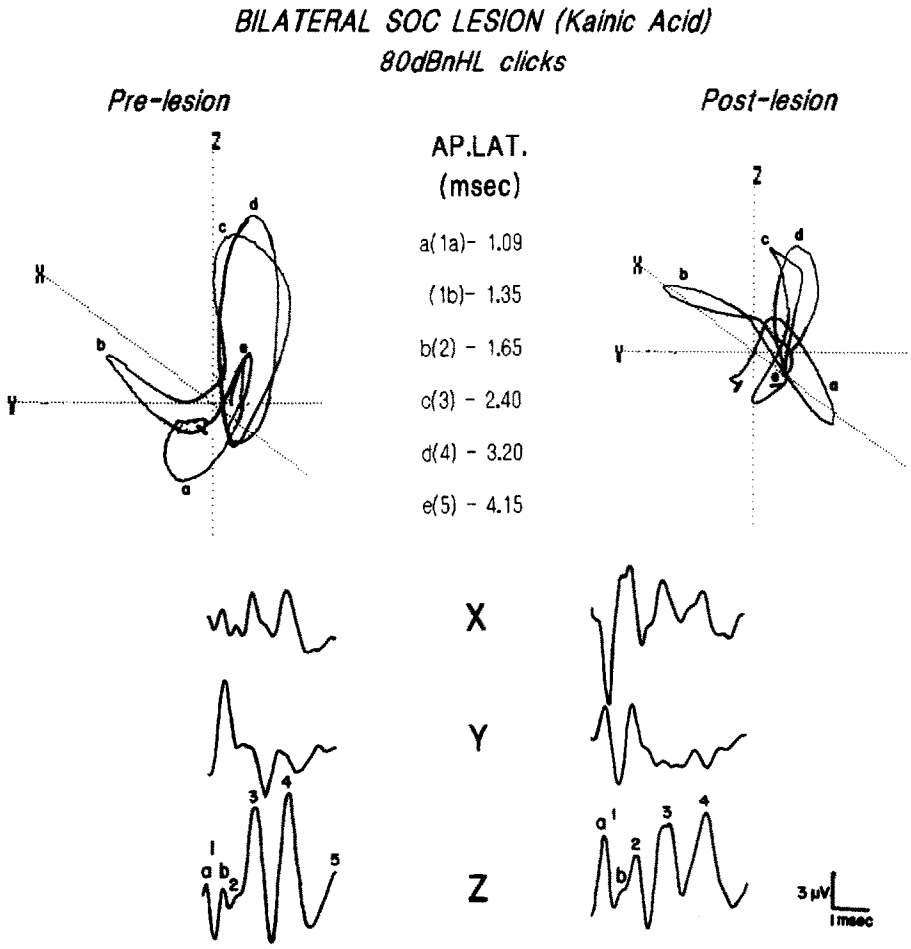

Fig. 6. 3CLTs in response to right ear stimulation from a cat with a bilateral neuronal destruction in the SOCs, before and after lesion induction. There are changes in apex orientation of 'a' and 'b', and amplitude reductions of 'c' and 'd'. Apex latencies (AP.LAT.) were the same for both records.

the preceding component 'c1'. These results are compatible with all subunits of SOC, bilaterally, contributing to the generation of 'd', with ipsilateral CN providing inputs to both SOCs.

Component 'e', corresponding to P5 of the 'Z' channel ABEP, was not affected by any of the neuronal lesions. The onset latency of it's planar segment was paradoxically decreased with the extent of myelin lesions in the vicinity of the ipsilateral MNTB and increased with myelin lesions in the vicinity of the MSO (Table V). The generators for this component are probably central to the trapezoid body and receive a diversity of inputs that travel in this fiber bundle.

The results of this study complement those of companion studies (Zaaroor and Starr, in press a, b) which analyzed a single-channel record (vertex – frontal sinus) from these same cats with neuronal lesions. Disagreements between the single-channel studies and the present study are few and revolve around the finding of a diminished amplitude in the single-channel record without an amplitude change in 3CLT. This discrepancy could result from changes in the equivalent dipole moment's orientation relative to the recording electrodes, and not necessarily from a reduction in total activity in the generator. For instance, neuronal lesions in the CN were associated with a

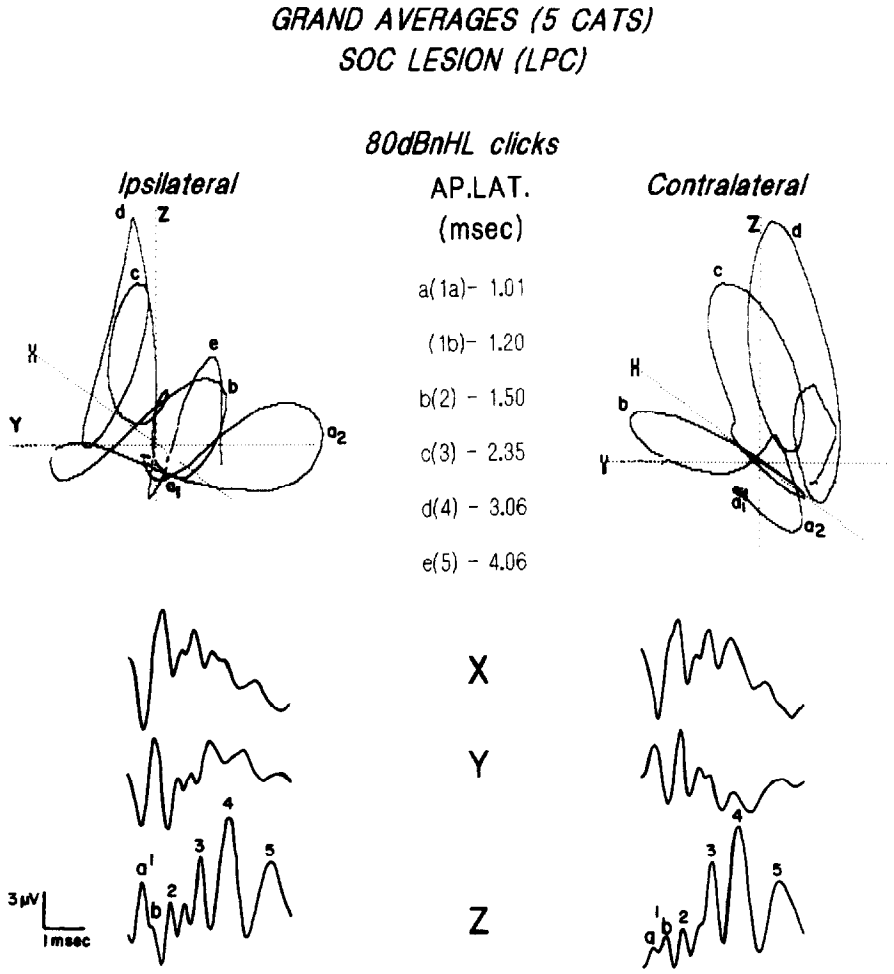

Fig. 7. 3CLTs to stimulation of the ear ipsi- and contralateral to restricted demyelination in the left trapezoid body, averaged across 5 cats. Only a minor orientational change of 'c' to ipsilateral stimulation is visible. Apex latencies (AP.LAT.) were the same for both records.

decrease in P1a amplitude in single-channel records (Zaaroor and Starr, in press b) while the present study only found an orientational change in 'a2' without amplitude reduction. The 3CLT results in the present study implicated MSO in the generation of 'd', both to ipsi and to contralateral stimulation, while the single-channel results did not. This difference may be a consequence of the different statistics used in the two studies. The single-channel study used linear regression analysis in which the extent of lesion to each nucleus was separately correlated with its effect on ABEP, while the present study used multiple regression analysis studying the effects of lesions to all structures in the same regression. In addition, the differences between studies may result from the sensitivity of 3CLT to the activity of generators with different orientations.

The unexpected findings of amplitude decrements and latency increases of P2, P3 and P4 in single-channel records to stimulation of the ear contralateral to a neuronal CN lesion were not all confirmed in the present study. 3CLT to contralateral stimulation showed only 'c2' to be delayed and 'd' to be reduced in amplitude. Such discrepancies between 3CLT and single-channel

TABLE IV

EXTENT OF LESIONS, IN PERCENT, IN EACH CAT

	AVCN	PVCN	DCN	MNTB	LSO	MSO
Kainic Acid Unilateral						
Cat 5				75	76	86
Cat 8				75	95	75
Cat 17				26	40	26
Cat 23				0	85	0
Cat 26				10	0	45
Cat 21	60	100	100			
Cat 24	31	74	24			
Cat 25	69	?	?			
Cat 28	91	74	79			
Cat 30	72	57	35			
Kainic Acid Bilateral						
Cat 20				64/82	100/100	99/100
Lyso. Phosph. Chol. Ipsilateral						
Cat 10						45
Cat 12				100	46	
Cat 13				26	47	
Cat 18					10	70
Cat 31				4	47	

In bilateral lesions, right/left extents are listed. LPC lesions to the trapezoid body are listed under the SOC nucleus injected. ? denotes missing data due to technical difficulties.
AVCN – anterior ventral cochlear nucleus; PVCN – posterior ventral cochlear nucleus; DCN – dorsal cochlear nucleus; MNTB – medial nucleus of the trapezoid body; LSO – lateral superior olivary nucleus; MSO – medial superior olivary nucleus.

TABLE V

SUMMARY OF SIGNIFICANT EFFECTS OF LESIONS IN FELINE BRAINSTEM ON 3CLT COMPONENTS, AS REVEALED BY MULTIPLE REGRESSION ANALYSIS

	AVCN	PVCN	DCN	MNTB	LSO	MSO
Kainic Acid Ipsilateral						
a3 LATa		+			+	
d LATa				+		
c1 AMPa				−	+	
d AMPa				−	+	+
Kainic Acid Contralateral						
c2 LATa	+					
d AMPa				−		+
Lyso. Phosph. Chol. Ipsilateral						
c2 AMPa				−		
e LATp				−		+

Significant increases are marked by +, decreases by −, while nonsignificance is indicated by an empty cell.
AVCN – anterior ventral cochlear nucleus; PVCN – posterior ventral cochclear nucleus; DCN – dorsal cochlear nucleus; MNTB – medial nucleus of the trapezoid body; LSO – lateral superior olivary nucleus; MSO – medial superior olivary nucleus; AMPa – apex amplitude; LATa – apex amplitude; LATp – plane onset latency.

analyses of ABEP following brainstem lesions have also been noted with midsaggital sections of the brainstem (Gardi et al., 1987).

The limited effects of myelin lesions on 3CLT components probably reflect the restricted spatial extent of the demyelination (Table IV) to the zone around the injected sites. The lesion never involved a significant portion of the fibers in the trapezoid body. In contrast, the neuronal lesions to CN and SOC were quite extensive in some animals. The failure to obliterate any of the components with neuronal lesions may reflect the bias of averaging the data together from all of the animals. Alternatively the generators of these components are complex, involving both neurones and fibers distributed spatially in the brainstem.

Acknowledgements

The expertise of Mr. J. Manago in preparation of histological sections and the indispensable support of the Anatomy Department of the University of California, Irvine are gratefully acknowledged.

TABLE VI

SUMMARY OF SIGNIFICANT EFFECTS OF LESIONS IN FELINE BRAINSTEM ON 3CLT APICES, AS REVEALED BY PAIRED *T*-TEST OF DIFFERENCES

3CLT	a1	a2	a3	b1	b2	c1	c2	d	e
Z Correlates		1a	1b	2		3		4	5
Kainic Acid Ipsilateral									
CN AMP				−		− −	−	−	
LAT				+		+	+	+	
SOC AMP								−	
Kainic Acid Contralateral									
SOC AMP							−		
Lyso. Phosph. Chol. Ipsilateral									
SOC AMP							− −		

Significant ($P < 0.001$) decreases are marked by − −, marginally significant ($P < 0.009$) increases by +, and decreases by −, while nonsignificance is indicated by an empty cell. Peaks in the 'Z' channel are placed under the 3CLT components corresponding in latency.

CN – lesion to cochlear nucleus; SOC – lesion to the superior olivary complex; AMP – apex amplitude; LAT – apex latency.

This work was supported in part by NIH Grant No. 11876.

Appendix 1 3CLT Analysis

Off-line analysis started with digital filtering of the evoked potentials to a bandpass of 100–3000Hz, followed by calculation of 3CLT measures from the 'X', 'Y' and 'Z' channels. 3CLT analysis was conducted by machine scoring algorithms as follows: To obtain orthogonality of the data, 'X' channel data were mathematically decomposed to their components in the Z direction and in the direction orthogonal to the Z/Y plane (which is the correct 'X' axis). This latter component was called 'corrected X' and replaced the original 'X' in all subsequent analyses. From the 'X' (corrected), 'Y' and 'Z' data, 3CLTs were obtained. Analysis of 3CLT included point-by-point (local) attributes, as well as segmental (global) properties of the trajectory in voltage space. Further details of our methodology were included in earlier reports (Har'El and Pratt, 1984; Pratt et al., 1985).

Points where Curvature, i.e., the local rate of bending of the trajectory in voltage space, reached locally (± 3 data points) maximal values were defined. The point-by-point amplitude attributes of the trajectory in voltage space were defined as the distance (in μV) of each point along the trajectory from the origin (zero potential in all channels) and was termed Trajectory Amplitude. Local Trajectory Amplitude maxima were noted, and when such a peak coincided (within 3 data points) with a Curvature maximum, the point of coincidence was called an apex. An apex was thus a point along the trajectory where bending, as well as the maximal absolute potential in any direction, were both maximal. Points with maxima in either Trajectory Amplitude or Curvature that were not coincident were not analyzed further. Apices were labeled alphabetically in the order of their appearance.

Once apices were defined, the extent of planarity near each apex was verified. We attempted to fit a plane to the data points in increasing ranges around each apex. In increasing the range around an apex, one point was added to the plane on one side, then to the other, and the point that added the least deviation from the new best fit plane was selected to be added. Fitting was conducted using a least-squares method, and the planar segement's boundaries were defined when the root-mean-square voltage (distance in voltage space) relative to the plane (Pratt et al., 1985) reached 0.1 μV. This criterion was chosen so that average deviations from the plane were within 5% of an average planar segment's dimensions (length or width). The results using this algorithm agree very well with manual definition of planar segments, based on visual inspection of deviations from the plane, as conducted in our, as well as other laboratories. The orientation of a planar segment is described by the 'sight vector', which is the line that is both orthogonal to the best-fit plane and passes through the origin. Planar segments can be described in terms of their orientation (A, B and C, which are the cosines of the angles of the 'sight vector' with the 'X', 'Y' and 'Z' analysis axes, respectively), position (D, the 'sight vector' length, i.e., the plane's distance from origin), the latencies of the planar segments' onset and end points, and their duration.

Because of the non-linear nature of the cosines used to define planar segment orientation, the

average orientation of planar segments, across subjects, cannot be calculated by averaging the individual cosines. In order to calculate the average orientation of planar segments, the coordinates of the 'sight vector' intersection with each best-fit plane were determined for each subject. The 'X', 'Y' and 'Z' coordinates, as well as the 'sight vector' length (D), which are all linear, were each averaged across subjects. The average orientation of the 'sight vector' was calculated by dividing the average 'X', 'Y' and 'Z' coordinates of 'sight vector' intersection with the plane, by the average length (D) of the 'sight vector'. These divisions produced the 'A', 'B' and 'C' values, respectively, of the average orientation of each planar segment. Intersubject variability of planar segment orientation was calculated in terms of angles ('included angles') by which individual planar segments deviated from the group average orientation. For each planar segment, a cone in voltage space within which 90% of individual prelesion orientations fell was determined, and was defined as the limit of normal orientation variability. Apex orientations were similarly analyzed, based on the apex's 'X', 'Y' and 'Z' coordinates and the trajectory amplitude of the apex (distance from origin at the apex).

References

Achor, L.J. and Starr, A. (1980a) Auditory brainstem responses in cat. I. Intracranial and extracranial recording. Electroenceph. Clin. Neurophysiol. 48, 154–173.

Achor, L.J. and Starr, A. (1980b) Auditory brainstem responses in the cat. II.Effects of lesions. Electroenceph. Clin. Neurophysiol. 48, 174–190.

Allen, A.R. and Starr, A. (1978) Auditory brainstem potentials in monkey (M. Mulata) and man. Electroenceph. Clin. Neurophysiol. 45, 53–63.

Buchwald, J.S. and Huang, C-M. (1975) Far field acoustic response: Origin in the cat. Science 189, 382–384.

Buchwald, J.S. (1983) Generators. In: E.J. Moore (Ed.), Bases of Auditory Brain-Stem Evoked Responses, Chapter 7, Grune and Stratton, New York, pp. 157–196.

Caird, D., Sontheimer, D. and Klinke, R. (1985) Intra- and extracranially recorded auditory evoked potentials in the cat. I. Source location and binaural interaction. Electroenceph. Clin. Neurophysiol. 61, 50–60.

Chimento, T.C., Williston, J.S., Jewett, D.L. and Gardi, J.N. (1987) The 3-channel Lissajous' trajectory of the auditory brain-stem response. VIII. Isolated frog sciatic nerve in a volume conductor. Electroenceph. Clin. Neurophysiol. 68, 380–385.

Coyle, J.T., Molliver, M.E. and Kuhar, M.J. (1978) In situ injection of Kainic Acid: A new method for selectively lesioning neuronal cell bodies while sparing axons of passage. J. Comp. Neur. 180, 301–324.

Curio, G., Oppel, F. and Scherg, M. (1987) Peripheral origin of BAEP wave II in a case with unilateral pontine pathology: a Comparison of intracranial and scalp records. Electroenceph. Clin. Neurophysiol. 66, 29–33.

Deupree, D.L. and Jewett, D.L. (1988) Far-field potentials due to action potentials traversing curved nerves, reaching cut nerve ends, and crossing boundaries between cylindrical volumes. Electroenceph. Clin. Neurophysiol. 70, 355–362.

Gardi, J.N., Sininger, Y.S., Martin, W.H., Jewett, D.L. and Morledge, D.E. (1987) The 3-Channel Lissajous' Trajectory of the auditory brain-stem response. VI. Effects of lesions in the cat. Electroenceph. Clin. Neurophysiol. 68, 360–367.

Gregson, N.A. and Hall, S.N. (1973) A quantitative analysis of the effects of the intraneural injection of lysophosphatidyl choline. J. Cell Sci. 13, 257–277.

Hall, S.M. (1983) The response of the (myelinating) Schwann cell population to multiple episodes of demyelination. J. Neurocytol. 12, 1–12.

Hall, S.M. and Gregson, N.A. (1971) The in vivo and ultrastructural effects of injection of Lysophosphatidyl Choline into myelinated peripheral nerve fibres of the adult mouse. J. Cell Sci, 9, 769–789.

Har'El, Z. and Pratt, H. (1984) Geometric analysis of short-latency evoked potentials. Math. Biosci. 69, 1–10.

Hashimoto, I., Ishiyama, Y., Yoshimoto, T. and Nemoto, S. (1981) Brainstem auditory evoked potentials recorded directly from human brainstem and thalamus. Brain 104, 841–859.

Jewett, D.L. and Williston, J.S. (1971) Auditory-evoked far fields averaged from the scalp of humans. Brain 94, 681–696.

Kano, Y., and Starr, A. (1987) Temporal relationship between single unit activity in superior olivary complex and scalp-derived auditory brainstem response in guinea pig. Brain Res. 419, 262–271.

Kimura, J., Mitsudome, A., Yamada, T. and Dickins, Q.S. (1984) Stationary peaks from a moving source in farfield recording. Electroenceph. Clin. Neurophysiol. 58, 351–361.

Legatt, A.D., Arezzo, J.C. and Vaughan Jr., H.G. (1986a) Short-latency auditory evoked potentials in the monkey. I. Wave shape and surface topography. Electroenceph. Clin. Neurophysiol. 64, 41–52.

Legatt, A.D., Arezzo, J.C. and Vaughan Jr., H.G. (1986b) Short-latency auditory evoked potentials in the monkey. II. Intracranial generators. Electroenceph. Clin. Neurophysiol. 64, 53–73.

Lev, A. and Sohmer, H. (1972) Sources of averaged neural responses recorded in animal and human subjects during cochlear audiometry (Electro-Cochleogram). Arch. Klin. Exp. Ohr. Nas. Kehlk. Heilk. 201, 79–90.

Martin, W.H., Jewett, D.L., Williston, J.S. and Gardi, J.N.

(1987a) The 3-Channel Lissajous' Trajectory of the auditory brain-stem response. III. Formation, analysis and reliability of planar segments in the cat. Electroenceph. Clin. Neurophysiol. 68, 333–340.

Martin, W.H., Jewett, D.L., Williston, J.S. and Gardi, J.N. (1987b) The 3-Channel Lissajous' Trajectory of the auditory brain-stem response. IV. Effects of electrode position in the cat. Electroenceph. Clin. Neurophysiol. 68, 341–348.

Møller, A.R. and Jannetta, P.J. (1982) Auditory evoked potentials recorded intracranially from the brain stem in man. Exp. Neurol. 78, 144–157.

Møller, A.R. and Jannetta, P.J. (1985) Neural generators of the auditory brainstem response. In: J.T. Jacobson (Ed.), The Auditory Brainstem Response, Chapter 2, Taylor and Francis, London, pp. 13–32.

Møller, A. and Burgess, J. (1986) Neural generators of the brain-stem auditory evoked potentials (BAEPs) in the rhesus monkey. Electroenceph. Clin. Neurophysiol. 65, 361–372.

Møller, A.R., Jannetta, P.J., Bennett, M. and Møller, M.B. (1981) Intracranially recorded responses from human auditory nerve: New insights into the origin of brain stem evoked potentials. Electroenceph. Clin. Neurophysiol. 52, 18–27.

Møller, A.R., Jannetta, P.J. and Sekhar, L.N. (1988) Contributions from the auditory nerve to the brainstem auditory evoked potentials (BAEP): Results of intracranial recording in man. Electroenceph. Clin. Neurophysiol. 71, 226–232.

Nakanishi, T. (1982) Action potentials recorded by fluid electrodes. Electroenceph. Clin. Neurophysiol. 53, 343–345.

Nunez, P.L. (1981) Electric Fields of the Brain. Oxford University Press, New York. pp. 100–101.

Ozdamar, O. and Delgado, R.E. (1990) Fiber tract model of auditory brainstem response generation using traveling dipoles. In: F. Grandori, M. Hoke and G.L. Romani (Eds.), Auditory Evoked Magnetic Fields and Electric Potentials, Advances in Audiology, Karger, Basel, 6, 194–206.

Picton, T.W., Hillyard, S.A., Krausz, H.I. and Galambos, R. (1974) Human auditory evoked potentials I. Evaluation of components. Electroenceph. Clin. Neurophysiol. 36, 179–190.

Plantz, R., Williston, J.S. and Jewett, D.L. (1974) Spatio-temporal distribution of auditory-evoked far field potentials in rat and cat. Brain Res. 68, 55–71.

Prasher, D.K. and Gibson, W.P.R. (1980) Brain stem auditory evoked potentials: significant latency differences between ipsilateral and contralateral stimulation. Electroenceph. Clin. Neurophysiol. 50, 240–246.

Pratt, H., Har'El, Z. and Golos, E. (1983) Three-channel Lissajous' trajectory of human auditory brain stem evoked potentials. Electroenceph. Clin. Neurophysiol. 56, 682–688.

Pratt, H., Har'El, Z. and Golos, E. (1984) Geometrical analysis of human three-channel Lissajous' trajectory of auditory brain-stem evoked potentials. Electroenceph. Clin. Neurophysiol. 58, 83–88.

Pratt, H., Bleich, N. and Martin, W.H. (1985) Three-channel Lissajous' trajectory of human auditory brain-stem evoked potentials. I. Normative measures. Electroenceph. Clin. Neurophysiol. 61, 530–538.

Pratt, H., Martin, W.H., Bleich, N., Kaminer, M. and Har'El, Z. (1987) Application of the three-channel Lissajous' trajectory of auditory brainstem-evoked potentials to the question of generators. Audiology 26, 188–196.

Rudell, A.P. (1987) A fiber tract model of auditory brain-stem responses. Electroenceph. Clin. Neurophysiol. 67, 53–62.

Scherg, M. (1984) Spatio-temporal modelling of early auditory evoked potentials. Rev. Laryngol. 105, 163–170.

Starr, A. and Squires, K. (1982) Distribution of auditory brainstem potentials over the scalp and nasopharynx in humans. Ann. NY Acad. Sci. 388, 427–442.

Starr, A. and Zaaroor, M. (1990) Eighth nerve contributions to cat auditory brainstem responses (ABR). Hear. Res. 48, 151–160.

Urbach, D. and Pratt, H. (1986) Application of finite impulse response digital filters to auditory brain-stem evoked potentials. Electroenceph. Clin. Neurophysiol. 64:269–273.

Von Monakow, C. (1914) Die Lokalisation im Grosshirn und der Abbau der Funktion durch kortikale Herde. Bergmann, Wiesbaden.

Wada, S-I. and Starr, A. (1983a) Generation of auditory brainstem responses (ABRs). I. Effects of injection of local anesthetic (Procain HCl) into the trapezoid body of guinnea pigs and cat. Electroenceph. Clin. Neurophysiol. 56, 326–339.

Wada, S-I. and Starr, A. (1983b) Generation of auditory brainsetm responses (ABRs). II. Effects of sugical section of the trapezoid body on the ABR in guinea pigs and cat. Electroenceph. Clin. Neurophysiol. 56, 340–351.

Wada, S-I. and Starr, A. (1983c) Generation of auditory brainstem responses (ABRs). I. Effects of lesions of pons and midbrain in guinea pigs. Electroenceph. Clin. Neurophysiol. 56, 352–366.

Williston, J.S., Jewett, D.L. and Martin, W.H. (1981) Planar-curve analysis of three-channel auditory brainstem response: a preliminary report. Brain Res. 223, 181–184.

Zaaroor, M. and Starr, A. (1991a) Auditory Brainstem Evoked Potentials in cat after kainic acid induced neuronal loss. I. Superior Olivary Complex. Electroenceph. Clin. Neurophysiol.

Zaaroor, M. and Starr, A. (1991b) Auditory Brainstem Evoked Potentials in cat after kainic acid induced neuronal loss. II. Cochlear Nucleus. Electroenceph. Clin. Neurophysiol.